Publication I

Self-assembly of cellulose nanofibrils by genetically engineered fusion proteins. Suvi Arola, Päivi Laaaksonen, Arja Paananen, Hanna Valo, Hendrik Hähl, Timo Laaksonen and Markus Ben Linder. *Soft Matter*, 2011, 7, pp. 2402–2411. DOI: 10.1039/c0sm01114b

Soft Matter

View Online
Dynamic Article Links

Cite this: DOI: 10.1039/c0sm01114b

www.softmatter.org

PAPER

Self-assembly of cellulose nanofibrils by genetically engineered fusion proteins†

Suvi Varjonen,[ab] Päivi Laaksonen,[a] Arja Paananen,[a] Hanna Valo,[c] Hendrik Hähl,[d] Timo Laaksonen[c] and Markus Ben Linder*[a]

Received 6th October 2010, Accepted 20th December 2010
DOI: 10.1039/c0sm01114b

One central problem for the function and manufacture of materials where performance relies on nanoscale structure is to control the compatibility and interactions of the building blocks. In natural materials, such as nacre, there are examples of multifunctional macromolecules that have combined binding affinities for different materials within the same molecule, thereby bridging these materials and acting as a molecular glue. Here, we describe the use of a designed multifunctional protein that is used for self-assembly of nanofibrillar cellulose. Recent advances in the production of cellulose nanofibrils have given inspiration for new uses of cellulosic materials. Cellulose nanofibrils have mechanical and structural features that open new possibilities for performance in composites and other nanoscale materials. Functionalisation was realised through a bi-functional fusion protein having both an ability to bind to cellulose and a second functionality of surface activity. The cellulose-binding function was obtained using cellulose-binding domains from cellulolytic enzymes and the surface activity through the use of a surface active protein called hydrophobin. Using the bi-functional protein, cellulose nanofibrils could be assembled into tightly packed thin films at the air/water interface and at the oil/water interface. It was shown that the combination of protein and cellulose nanofibrils resulted in a synergistic improvement in the formation and stability of oil-in-water emulsions resulting in emulsions that were stable for several months. The bi-functionality of the protein also allowed the binding of hydrophobic solid drug nanoparticles to cellulose nanofibrils and thereby improving their long-term stability under physiological conditions.

1 Introduction

One principal approach for improving performance in materials is through control of their structure and interactions at levels of hierarchy from molecular to macro level. By fabricating nanocomposites and nanostructured materials, improvements in toughness and strength of materials, new possibilities for drug delivery, biocompatibility, adhesion, *etc.* can be achieved.[1–4] One material attracting much interest is cellulose. Wood is a natural composite consisting of cellulose, hemicellulose, lignin, and some other minor components. Cellulose is a polymer formed by the repeating units of β-(1–4)-D-glucopyranose. The polymer chains are packed into fibrils that have cross-sectional dimensions of 3–20 nm and which are typically considered as the lowest level of hierarchy in cellulose assembly.[5] As a part of the cell wall structure, these fibrils are called microfibrils. Recently, methods have been developed to disintegrate wood into the elemental microfibrils producing a material referred to as "nanofibrillar cellulose" (NFC) as a separate fraction.[6,7] NFC preparations are largely free from the other cell wall components. In this context, the term nanocellulose has also been adapted.[8,9] Depending on how the materials is produced, one can also obtain "cellulose nanocrystals" (CNC, also called cellulose nanowhiskers).[10] The main difference between the two forms is the aspect ratio, NFC can have lengths of several micrometres, whereas CNC are shorter, typically some hundreds of nanometres in length.

NFC shows promise as a novel material allowing technical solutions in a sustainable way. The long and entangled fibrils make NFC a good rheology modifier[6] and material for functional aerogels.[11] The fibrils have a high aspect ratio and excellent mechanical properties. Therefore NFC is an attractive component for reinforcement of composite materials.[7,12,13] However, to achieve a sufficient compatibility between the NFC and polymer, covalent modifications of the NFC have been required. Covalent modifications have some drawbacks such as need for solvent exchange and weakening or disintegration of the fibrils,[14] thereby loosing some of the potential advantages of NFC.

[a]*VTT, Technical Research Centre of Finland Biotechnology, Tietotie 2, FIN-02044VTT, Finland. E-mail: markus.linder@vtt.fi*
[b]*Department of Applied Physics, Aalto University School of Science and Technology, P.O. Box 15100, FI-00076 Aalto, Finland*
[c]*Division of Pharmaceutical Technology, University of Helsinki, P.O. Box 56, FI-00014, Finland*
[d]*Department of Experimental Physics, Saarland University, 66041 Saarbrücken, Germany*

† Electronic supplementary information (ESI) available: Further data on characterization and rheology. See DOI: 10.1039/c0sm01114b

One major challenge for the use of NFC and CNC is therefore to functionalise their surfaces in precise and desired ways. Through functionalisation we aim at achieving compatibility with other components, adhesiveness, or self-assembly. In this work we functionalised cellulose nanofibrils so that they would spontaneously assemble at interfaces or interact with other components through interfacial interactions. We aimed at a biomimetic approach using self-assembly rather than using covalent modification. Such functionalisation was realised using a bi-functional (or two-block) polymer. In nature, the strategy to use bi-(or multi-) functional proteins is for example found in materials such as nacre.[15] In this example, the proteins have the property of binding to both major components of nacre, aragonite and chitin, thereby acting as cross-linkers. In our approach, one block had affinity towards cellulose and the other was amphiphilic (or lipophilic). In this way, an amphiphilic function could be attached to the NFC. This polymer was made by fusing the proteins together into a single polypeptide chain by genetic engineering (Scheme 1). The cellulose-binding function was obtained through specialised cellulose-binding domains, CBDs (also called cellulose-binding modules, CBMs), and the amphiphilic (surface active) function through an amphiphilic protein called hydrophobin (a class II hydrophobin, HFBI).

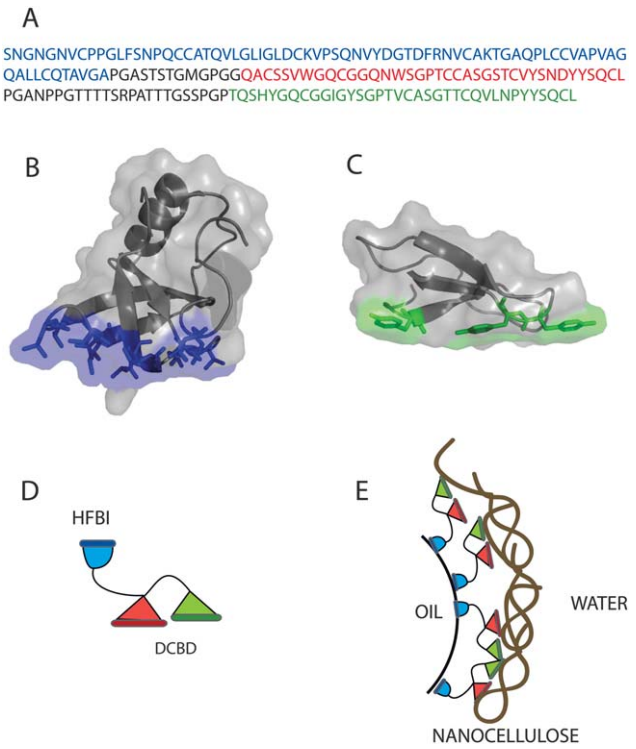

Scheme 1 (A) Amino acid sequence of the fusion protein used to functionalise cellulose. The amphiphilic protein HFBI is first in the sequence (blue), followed by two cellulose-binding sequences Cel6A-CBD (red), and Cel7A-CBD (green). The two CBD sequences are very similar in both structure and function. The domains are separated by linkers (black) to allow flexibility. (B) Structure of HFBI. The hydrophobic patch that makes the protein amphiphilic is shown in blue (PDB id 2FZ6).[38] (C) Structure of the Cel6A-CBD. The aromatic side chains that bind cellulose are show in green (PDB id 1CBH).[39] (D) Cartoon of the HFBI–DCBD fusion protein. The blue part represents HFBI, and the two CBDs (Cel6A-CBD (red), and Cel7A-CBD (green)) form the "double-CBD" (DCBD) part. (E) Schematic illustration of how the interactions of the fusion protein can lead to the assembly of nanocellulose on oil (or air)–water interfaces through the combination of interface (HFBI) and cellulose (DCBD) binding.

CBDs are non-catalytic parts of enzymes that degrade cellulose and plant materials.[16,17] These enzymes typically have a two-domain structure where the CBD is linked to the catalytic domain through an extended linker. The role of the CBDs is to bring the catalytic part of the enzyme close to the cellulose surface.[18] CBDs can be produced as individual polypeptides or they can be genetically fused to other proteins, *e.g.* to immobilise these to a cellulose matrix.[19] In this work, we used fungal CBDs that have a size of about 40 amino acids and bind to cellulose through one face of the molecule, which has three characteristic aromatic residues (Scheme 1). This cellulose-binding face has a length of about 3 nm.

Hydrophobins are amphiphilic proteins produced by filamentous fungi.[20–22] They are often secreted in large amounts and have several different functions as surfactants and adhesive agents in different stages of fungal growth and development. The surface activity and self-assembly of hydrophobins at interfaces are extraordinary in many ways, for example in the stable films and foams that they can form.[23,24] The surfactant properties have also been used to coat and make nanoparticles of compounds having low solubility in aqueous solution.[25] The structure of the hydrophobin used here (HFBI) shows that the protein is almost spherical and has a typical amphiphilic structure with one face of the protein consisting only of aliphatic hydrophobic side chains and the rest of the protein showing a polar surface typical for soluble proteins (Scheme 1). The HFBI-hydrophobin has a size of approximately 70 amino acids and a cross-section of about 2 nm.

In this study the functionality of this fusion protein was studied extensively to understand its interactions with cellulose and at interfaces. The fusion protein was then used in the formation of emulsions and for attaching drug nanoparticles to NFC. The goal was to study whether it was possible to bring cellulose nanofibers in a controlled manner to air/water, oil/water or solid/water interfaces by utilising the bi-functional engineered protein, HFBI–DCBD, and to study how the overall properties of the system could be affected in this manner.

2 Experimental

2.1 Production and preparation of cellulose nanofibrils (NFC) and cellulose nanocrystals (CNC)

NFC were prepared by mechanical disintegration of bleached birch pulp by ten passes through a M7115 Fluidiser (Microfluidics Corp.), essentially according to previous reports.[6] The solid content of the prepared water dispersion was 1.7%. The amount of hemicellulose (mainly xylan) in the final NFC dispersion was approximately 25–28%. For some experiments larger aggregates of NFC were removed by centrifugation. Samples were first sonicated (Soniprep 150 MSE, amplitude 24 μm, 10 minutes). After centrifugation (Beckmann Optima LE-80K, TFT 65.38 rotor, 10 000*g*), the cellulose retained in the supernatant was collected. The cellulose concentration was 0.6 g l^{-1} as determined gravimetrically.

CNC were prepared as described previously[26,27] using Whatman 541 ash-less filter paper (Whatman, UK) as the starting material. The cellulose nanocrystals were partially hydrolysed in 4 M HCl at 80 °C for 225 minutes.

2.2 Production and purification of HFBI, HFBII, and HFBI–DCBD

The bi-functional fusion protein consisted of one hydrophobin part linked to two different CBDs in series (sequence in Scheme 1A). The HFBI-hydrophobin from *Trichoderma reesei*[28] was used and the two CBDs were from the enzymes Cel7A (previously CBHI)[29] and Cel6A (previously CBHII),[30] also from *T. reesei*. These modules of the proteins were connected by polypeptide linker regions as previously reported[31] and shown in Scheme 1. The abbreviation HFBI–DCBD was used for the fusion protein. The fusion protein was produced by recombinant means in *T. reesei* and purified by aqueous two phase extraction as described previously.[31] The protein was then purified by preparative reversed phase high performance liquid chromatography (RP-HPLC) using a water acetonitrile gradient with 0.1% trifluoro acetic acid. The identity and concentration were verified by amino acid analysis. Mass spectroscopy was used to verify the identity. HFBI and HFBII were produced using recombinant strains of *T. reesei* and purified by RP-HPLC as described previously.[32] All proteins were lyophilised before use.

2.3 Preparation of ^{3}H-labelled HFBI–DCBD

HFBI–DCBD was labelled with tritium for interaction studies by reductive methylation as reported previously.[33,34] 1.9 mg of lyophilised HFBI–DCBD was dissolved in 1.9 ml of 0.2 M borate buffer, pH 8.96 and cooled on an ice bath. 13.2 μl of 0.37% formaldehyde and 100 mCi of ^{3}H enriched $NaBH_4$ (10 Cimmol^{-1}, NET023H100MC, PerkinElmer) in 150 μl of 0.01 M NaOH were added and mixed for 30 minutes. The reaction was terminated by RP-HPLC. The specific activity was 0.40 Ci mmol^{-1}.

2.4 Determination of binding isotherm of HFBI–DCBD to NFC

A 100 μM stock solution of HFBI–DCBD containing 1% ^{3}H-labelled HFBI–DCBD in 50 mM acetate buffer (pH 5.0) with 1.37 mM HFBII was prepared. Solutions with different fusion protein concentrations were made from the stock solution by diluting with the same buffer containing 1.37 mM HFBII. The excess HFBII was used to minimise nonspecific binding of the fusion protein to test tube walls and filters. 200 μl of each protein solution was mixed with 200 μl of 1 g l^{-1} NFC in MilliQ-water and stirred in ambient temperature for 1 h. Before mixing NFC with the protein solution it was dispersed with a tip ultrasonicator (Soniprep 150 MSE, 5 minutes, amplitude 24 μm). After equilibration, the suspension was filtered through a disposable filter (Millipore, Millex®-GV filter unit, PVDF, hydrophilic, 0.22 μm, 13 mm, non-sterile) and the amount of free HFBI–DCBD was determined by liquid scintillation counter (Pharmacia, Wallac 1410) from the filtrate.

2.5 Determining the stability of the HFBI–DCBD binding to NFC

A series of identical mixtures of NFC and HFBI–DCBD containing ^{3}H-labelled HFBI–DCBD were first prepared (500 μl). The equilibrium concentration of bound protein was determined from two samples to determine the initial equilibrium point on the isotherm. The other samples were then diluted with buffer (containing no HFBI–DCBD). Dilutions from two- to ten-fold were used. The samples were filtered at different time points and analysed to determine possible release of bound protein. HFBI–DCBD was quantified from both supernatant and cellulose. To separate cellulose and supernatant, the mixture was filtered (0.22 μm Durapore membrane, Millipore). When the protein was quantified from the cellulose fraction, the filter was washed to remove unbound protein from the sample.

2.6 Formation and characterisation of monolayers on the langmuir trough

Monolayer isotherms were measured and Langmuir–Schaefer (LS) films were prepared using a KSV Minimicro trough (KSV Instruments). We use the term LS films to describe molecular layers that have transferred from the air/water interface by touching the surface with a hydrophobic material. In LS films therefore the outermost side will be the side of the surface layer that was directed towards the bulk water during film assembly. The layers were prepared by injecting protein solution, a mixture of protein and nanocellulose or solution containing only nanocellulose onto the air/water interface. The samples contained 6.25 to 25 μM protein and 0.5 to 2 g l^{-1} of NFC or CNC. After stabilisation (20–30 min), the isotherm of the monolayer was recorded by a constant rate compression of 3 mm min^{-1} at a constant temperature of 21 °C. The nanocellulose containing samples were dispersed with a tip ultrasonifier (Soniprep 150 MSE, 2 minutes, amplitude 24 μm). Samples containing only protein were dispersed mildly in an ultrasonic bath (Sonoswiss, SW3) for 30 seconds.

LS-films were prepared by first compressing the monolayer to a surface pressure of 30 mN m^{-1}. The surface films were then deposited onto pieces (10 × 10 mm) of freshly cleaved, ZYA quality, highly oriented pyrolytic graphite (HOPG), (NT-MDT Europe BV). HOPG was found suitable because it has a very flat hydrophobic surface. The LS films were then carefully rinsed with water to remove excess protein and unbound nanocellulose and dried in a vacuum desiccator.

2.7 Atomic force microscopy

Atomic force microscopy (AFM) was used to image LS films. A NanoScope IIIa Multimode (E-scanner, Digital Instruments/Veeco) AFM instrument was used with an NSCI5/AlBS cantilever (μMASCH). All images were recorded in tapping mode in air with scan rates of 0.8–1 Hz (free amplitude was about 0.65 V). The damping ratio was around 0.7–0.85. Images were flattened to remove possible tilts in the image data.

2.8 Interfacial dilatational rheology

Dilatational rheology of the protein film, NFC film or films containing both components was studied at air/water and oil/water interfaces by an oscillating air bubble or pendant drop, respectively. Measurements were carried out by injecting an air bubble into aqueous solution containing the components under study. For oil/water interface measurements a droplet of the aqueous solution was suspended from a capillary immersed in hexadecane (Sigma-Aldrich). The droplet volume was oscillated in a sinusoidal form using a pulsating drop module (KSV PD 100, KSV Instruments Ltd.). Before rheological measurement, the interfacial tension was followed until equilibrium was reached (CAM 200, KSV Instruments Ltd.). At equilibrium, pulsation of the droplet volume at 0.1 Hz was started. The surface area and tension of the droplet were determined by recording a few oscillations at a time and by repeating the measurement a few times with several minutes interval. Rheological parameters were determined from the data with the instruments own software (OscDrop2008, KSV Instruments Ltd.).

2.9 Preparation of emulsions

Emulsions were prepared from pure hexadecane and water solutions containing different amounts of HFBI–DCBD protein, nanocellulose or combinations thereof. The volume fraction of hexadecane was kept as 10% and the total volume of the emulsions was 1 ml. Emulsions were formed by ultrasonication of mixtures of oil and water phase with an ultrasonic probe (Soniprep 150 MSE, amplitude 26 μm) for 4 × 30 seconds in an ice bath, followed by homogenisation in an ultrasonic bath for 1 hour. Creaming of the emulsions was studied by following the phase separation after homogenisation. The final volume fraction of emulsion phase was determined from separation of the clear aqueous phase from the opaque emulsion phase, observed using a digital camera.

2.10 Epifluorescence and confocal microscopy

The structure of the emulsions was studied by staining cellulose or hexadecane with fluorescent dyes. Nanocellulose was imaged by epifluorescence microscopy (Olympus BX-50) by staining cellulose with Calcofluor (Scandinavian Brewery Laboratory Ltd.) and imaging fluorescence. More information on the 3-dimensional structure of the emulsions was obtained by confocal microscopy (Radiance Plus, BIO-RAD). For verification of formation of an oil-in-water emulsion, an oil soluble stain, Nile Red (Molecular Probes), was added to the samples prior to imaging. A blue argon laser (488 nm) was used for excitation of the dye.

2.11 Drug nanoparticle preparation and binding to cellulose

An anti-solvent precipitation technique was used to form nanoparticles of a hydrophobic drug, itraconazole (ITR, Apotecnia Murcia, Spain) and hydrophobins as described previously.[25] Tetrahydrofuran (THF, p.a., Riedel-de Haën, Germany) was used as the solvent for ITR. HFBI, HFBII or HFBI–DCBD was first dissolved in water (0.6 g l^{-1}). The solution was sonicated and placed on ice. The ITR solution (12 g l^{-1}) was filtered with PVDF syringe filters (PALL, Ann Abor, USA) to remove possible dust particles. The ITR (0.25 ml) solution was rapidly added into the hydrophobin solution (5 ml). The receiving liquid was stirred vigorously with a magnetic stirrer and the temperature of the solution was controlled by keeping the sample on ice. A white precipitate was observed as a turbid solution immediately after ITR addition, indicating the formation of the nanoparticles. The solution was stirred for 20 min.

NFC was used at a concentration of 8.4 g $l^{-1}$and sonicated immediately prior to use. Nanoparticle suspensions were mixed with NFC solution to a final ITR : HFB : NFC weight ratio of 1 : 1 : 2. The ionic strength was adjusted by adding NaCl up to 300 mM. The suspensions were shaken at room temperature for 20 min before taking the first TEM samples. Characterisation of the particle size and morphology was done by transmission electron microscope (FEI Tecnai F12, Philips Electron Optics, The Netherlands). Nanoparticle dispersions were dried on formvar film-coated copper grids with mesh size 300 (Agar Scientific, Essex, UK).

3 Results and discussion

3.1 The binding isotherm for HFBI–DCBD to NFC

The affinity and capacity of HFBI–DCBD binding to NFC were determined (Fig. 1). Data were fitted using a one-site binding Langmuir adsorption model (Graph Pad, CA, USA). The affinity constant, K_d, was 2.4 μM and the binding capacity 20 μmol g^{-1}. These values are very close to previously observed ones for the binding of an individual DCBD-construct on bacterial cellulose. It was previously shown that placing two CBDs in tandem results in a synergic increase in the binding affinity compared to using individual CBDs.[35] This was the reason for choosing the DCBD as the fusion partner. The capacity converted to mass units was 0.37 g of HFBI–DCBD per gram of NFC.

The DCBD binding functionality of HFBI–DCBD was also studied using a quartz crystal microbalance (QCM, see ESI†). Injection of HFBI solution over a polystyrene (PS) surface leads to the formation of a monomolecular layer of hydrophobin, attached to the surface as described previously.[36] This was

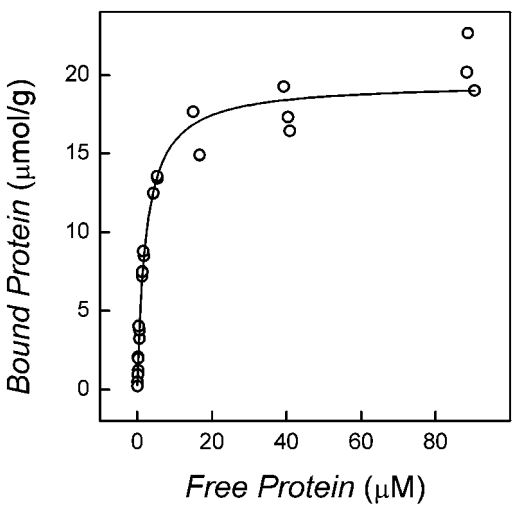

Fig. 1 Binding isotherm of HFBI–DCBD on nanofibrillar cellulose. K_d of the binding of HFBI–DCBD to NFC is 2.4 μM and the binding capacity of NFC is 20 μmol of HFBI–DCBD per gram.

observed in the QCM sensograms for both HFBI and the HFBI–DCBD fusion proteins as increase of mass of 200 ng cm^{-2} for HFBI and 650 ng cm^{-2} for HFBI–DCBD monolayer, corresponding to mean molecular areas of ~6.3 nm^2 for HFBI and ~4.7 nm^2 for HFBI–DCBD (see Fig. S3†). After rinsing with buffer, CNC was injected. The mass bound to the HFBI layer was 900 ng cm^{-2} whereas HFBI–DCBD bound approximately 3 μg cm^{-2}. The masses of CNC layers are only rough estimates due to limitations of the QCM method (discussed in the ESI†). It appears that the monolayer of HFBI is able to bind some CNC non-specifically or that a small amount of CNC sediments on the sensor chip. However, the amount of CNC that binds to the fusion protein is significantly higher than the mass bound to HFBI, showing a specific interaction between CNC and the CBD units.

3.2 Non-equilibrium desorption of HFBI–DCBD from NFC

We investigated the rate of release of HFBI–DCBD from cellulose to understand how stable the modification would be under changing conditions. Mixtures of HFBI–DCBD and NFC were first equilibrated and then diluted with buffer, increasing the volume to 2–10 times the original. If the binding of HFBI–DCBD to NFC would be reversible, a dilution of the sample should result in the formation of a new equilibrium point along the binding isotherm in a time comparable to the binding event. If binding were irreversible or show a very slow desorption, the concentration of free protein should decrease due to the dilution, but the amount of cellulose-bound protein would have remained essentially unchanged. The results showed that in two hours, only a little HFBI–DCBD desorbed from the cellulose in diluted samples and thus desorption was slow (Fig. 2). Over 96% of the bound protein remained bound when the equilibrated NFC/protein suspension was diluted by a factor of 2 and allowed to reach a new equilibrium (data not shown) and over 80% was found bound after dilution by a factor of 10. The amount of bound protein was found to decrease slightly with time with the greater dilution and after 20 minutes of incubation in room temperature. The amount of HFBI–DCBD was measured both as bound to cellulose and as free in solution. Both ways of measuring gave the same results.

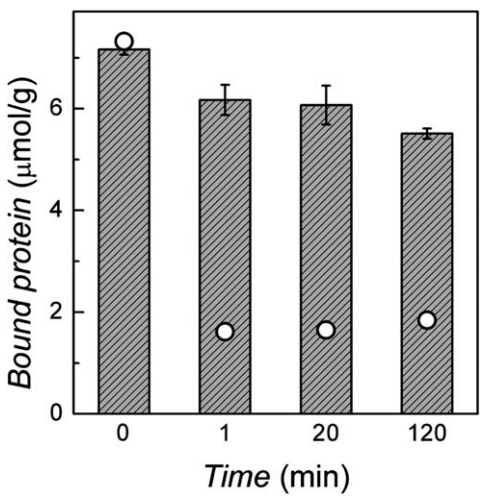

Fig. 2 Summary of dilution driven desorption of HFBI–DCBD from NFC. The columns represent the measured amount of bound HFBI–DCBD per gram of NFC. Time 0 corresponds to the situation before the 10× dilution. After dilution the amount of cellulose bound HFBI–DCBD was measured at times 1, 20 and 120 minutes (columns). The open circles show how much bound protein is expected based on the adsorption binding curve (Fig. 1). The observed bound amount of HFBI–DCBD decreases only slightly showing that the desorption kinetics is very slow. The initial concentration of HFBI–DCBD was 5 μM.

3.3 Formation of self-assembled films

The functionality of the HFBI–DCBD fusion protein at the air/water interface was investigated by studying its behaviour in combination with NFC in a Langmuir trough.[37] In Fig. 3, the surface pressure–area isotherms for the interfacial protein films are shown. The HFBI–DCBD fusion protein showed a slightly lower mean molecular area of ~1.8 nm^2 than the HFBI control which was ~2.6 nm^2. The reason is not directly evident since the bulkier DCBD part could be expected to increase the molecular dimensions. However, since the DCBD fusion part increases the size of the hydrophilic part of the fusion protein, the reason may be a decreased tendency to assemble at the surface, or different packing arrangements (AFM images of surfaces in Fig. S1, ESI†).

The formation of monolayers at the air/water interface was also studied by ellipsometry to verify the results (see Fig. S2†). The experiments showed that both proteins formed a full monolayer at the air/water interface even without compression. The mean molecular areas from ellipsometry measurements were ~3.6 nm^2 and ~6.0 nm^2 for HFBI and HFBI–DCBD respectively, which are very close to the crystallographic dimensions of the proteins.[38,39] The differences in the mean molecular areas obtained by Langmuir trough and ellipsometry can be caused by the differences in the preparation of the interfacial film. In ellipsometry the interfacial film is formed by free adsorption of the protein from the bulk and in Langmuir trough the protein is

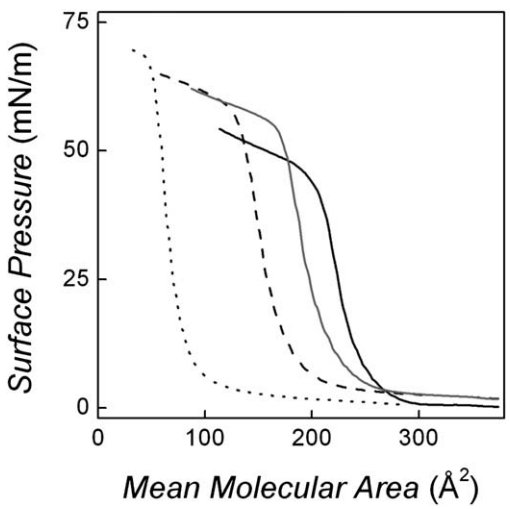

Fig. 3 Isotherms of the interfacial molecular films at air/water interface. The surface pressure as a function of the mean molecular area of HFBI (solid line), HFBI–DCBD (dashed line), 1 : 1 molar ratio mixture of HFBI and HFBI–DCBD (gray line) and the combination of HFBI–DCBD and NFC (dotted line) measured at 21 °C. Mean molecular area was calculated from the amount of injected protein.

injected dropwise onto the interface and compressed to form the film. By compressing the film it is possible that a denser arrangement of protein in the film is achieved and thus a smaller value for mean molecular area compared to ellipsometry. In ellipsometry the proteins are adsorbing freely from the bulk and thus the DCBD part of the fusion protein can interfere in the adsorption of the fusion protein and lead to a larger mean molecular area compared to HFBI.

Addition of nanocellulose (NFC or CNC) to HFBI–DCBD before film formation resulted in changes in the surface pressure–area isotherms compared to only HFBI–DCBD (Fig. 3, data for CNC not shown). The film was prepared from a mixture of 25 μM HFBI–DCBD and 0.5 mg ml^{-1} NFC. In these conditions, ~30% of the protein adsorbed to NFC and the concentration of the free protein remaining was ~17 μM. The surface pressures for film collapse of the NFC containing film were slightly higher than those of the protein films, but the presence of NFC was not otherwise observable in experiments using the Langmuir trough. On the other hand, binding of the protein decreased the amount of free protein at the interface shifting the isotherm towards smaller molecular area (~30% was bound to cellulose at these conditions). To analyse how NFC had been incorporated in the interfacial film, samples of the surface films were deposited on HOPG using the LS technique and imaged by AFM, as described above. As seen in Fig. 4A, a mesh of nanocellulose fibrils has packed as a thin layer on top of the protein film. The NFC density was not uniform across the interfacial film. Similar results were obtained for CNC, as seen in Fig. 4B. Control experiments with only NFC or CNC (lacking protein) did not result in any sort of interfacial film.

3.4 Rheology of the fusion protein/nanocellulose surface films

Surface shear rheological properties of self-assembled films of protein and its combination with NFC at air/water interface were investigated next. In surface shear rheological measurements, the viscoelastic moduli of HFBI and HFBI–DCBD at constant shear and frequency were followed as a function of time (Fig. S4†). Results showed that the interfacial film of HFBI–DCBD formed slower and had smaller moduli than HFBI. Elastic moduli, G', were dominant for all studied interfacial films indicating that they are elastic rather than viscous in nature. The high G' value, ~1.2 N m^{-1}, obtained for HFBI was comparable to the one previously reported in literature.[21,24] The G' value for HFBI–DCBD, ~0.2 N m^{-1}, although an order of magnitude lower than that for HFBI, it is high compared to other proteins reported in literature.[40,41] The high values of rheological moduli for wild type HFBI are most likely due to the mechanism by which the hydrophobin functions, that is through strong lateral interactions between the molecules. For HFBI–DCBD, the values are significantly lower probably because the normal functional tight packing of the HFBI is sterically hindered by the DCBD fusion partner. A contributing effect for the decrease in G' value for HFBI–DCBD can also be an altered interfacial packing arrangement as compared to HFBI. By ellipsometry, it is seen that the packing density is different for HFBI–DCBD and HFBI, showing mean molecular areas of ~6 nm^2 and ~3.6 nm^2 respectively. It can therefore be expected that the interactions of the molecules are different at the interface, explaining the differences in the G' value. The differences in the adsorption rates for HFBI and the fusion protein are probably due to the size difference of the proteins (HFBI–DCBD ≈ 18 500 Da, HFBI ≈ 7200 Da), giving a significant lowering of the diffusion rate of the larger molecule.

Addition of NFC to the interfacial HFBI–DCBD film caused a slight increase in viscoelastic moduli, but also a large increase in the variation between measurements (See, Fig. S4–S7, ESI†, and Table S1†). The absolute moduli of the hybrid film containing both HFBI–DCBD and NFC do not significantly differ from the values for the film of HFBI–DCBD only indicating that the protein forms a stable interfacial layer, which the NFC does not disturb. However, the deviation of measured curves increases, probably due to variation in the density of NFC fibrils that are attached to the HFBI–DCBD film at the interface.

Dilatational surface rheology of HFBI–DCBD ± NFC hybrid films at air/water and hexadecane/water interfaces was studied by an oscillating pendant drop method. Initially equilibrium was allowed to form. Assembly of HFBI–DCBD led to a significant decrease of surface tension at air/water interface, from initial ~72 mN m^{-1} to final 55 mN m^{-1}. Similarly values decreased from 30 mN m^{-1} to 9 mN m^{-1} at the oil/water interface. Adsorption of NFC to the interfaces did not decrease the interfacial tension as much as the protein did (see Table 1). Under these conditions, ~7% of the protein was bound to the cellulose (calculated from the binding isotherm (Fig. 1)). The values of dilatational moduli for pure NFC at oil/water interface are significantly larger than the ones at air/water interface, which implies that NFC itself has a tendency to adsorb at the oil/water interface.

Dilatational rheological measurements are summarised in Table 1. A low phase lag was observed for all the film types, implying the formation of elastic films. At the air/water interface,

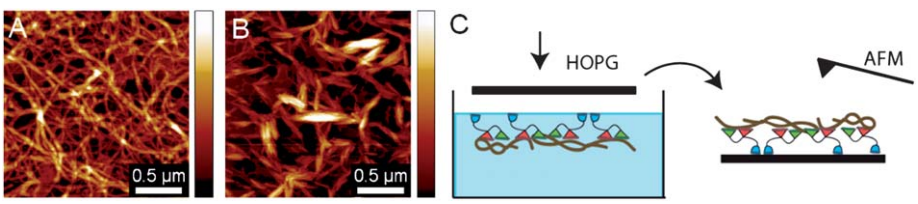

Fig. 4 AFM topography images of self-assembled protein/cellulose films picked up from air/water interface at surface pressure 30 mN m^{-1}. (A) An interfacial film formed from a combination of HFBI–DCBD and NFC. (B) An interfacial film formed from a combination of HFBI–DCBD and CNC. In both cases a well-defined two-layered hierarchical structure was obtained. The height scale in both images is 30 nm. (C) Schematic representation of how samples were prepared. First the fusion protein was allowed to assemble on the air/water interface together with NFC or CNC. Then the surface layer was lifted off from the surface by touching with a piece of HOPG. HOPG with the surface layer attached was then imaged with AFM.

Table 1 Values of interfacial tension, viscoelastic moduli and phase lag at air/water and hexadecane/water interfaces in the presence of 0.1 gl^{-1} HFBI–DCBD protein, light fraction of NFC and their combination

	Surface/interfacial tension/mN m^{-1}	$\|E\|$/mN m^{-1}	E'/mN m^{-1}	E''/mN m^{-1}	Phase lag/deg
HFBI–DCBD (air/w)	57	235	234	6	−1
HFBI–DCBD (o/w)	9	33	32	5	8
NFC (air/w)	63	8	8	0	1
NFC (o/w)	15	21	20	4	11
HFBI–DCBD + NFC (air/w)	53	146	145	16	6
HFBI–DCBD + NFC (o/w)	9	14	14	1	5

the value of dilatational elastic modulus E' was very high for pure protein, but low for pure NFC. NFC together with protein had intermediate E' values. HFBI results were comparable to earlier observations from a Langmuir trough method.[41] At the oil/water interface the absolute moduli values were much smaller and samples with only protein had the highest values. The behaviour of the hybrid film at the oil/water interface deviated from the air/water interface and showed the lowest E' value. This is probably due to NFC's different behaviour at the two interfaces. Since NFC was observed to form a film at the oil/water interface, there may be competitive adsorption of NFC and HFBI–DCBD leading to less-ordered film than at the air/water interface, where formation of a stable hydrophobin layer is very favourable and practically no NFC adsorption was observed. A reason for the assembly of NFC might be their high surface energy, which makes them very sensitive towards other solvents than water. It has been shown that the dispersed nanofibrillar structure may collapse in the contact with organic solvents.[42] On the other hand, low elastic moduli of the protein/NFC films imply to restricted dilatation of the film containing cellulose. The interface between pure water and hexadecane was studied as a reference and was also elastic in nature, but had a lower modulus $|E|$ than the other interfaces.

We conclude that the NFC alters the rheological properties of interfacial films to some extent but that the properties are still dominated by the properties of hydrophobin.

3.5 NFC and HFBI–DCBD as emulsion stabilisers

Emulsions of hexadecane and water in the presence of HFBI–DCBD and/or nanocellulose were studied. As shown above the self-assembly of HFBI–DCBD and NFC led to interfacial films and we investigated how the possible formation of such films could affect the properties of emulsions. Effects could include the stabilisation of interfaces, and thereby increased stability of emulsions. Emulsion structures were studied by microscopy and they were confirmed to be of oil-in-water type by staining the oil phase with a lipophilic dye (Nile Red) (see Fig. S8 and S9†). Oil droplets could also be observed by bright field microscopy and their size varied from tens of micrometres to some hundreds of nanometres for different samples and emulsion types. Fig. 5A shows an example of an emulsion formed by NFC alone. NFC is stained with Calcofluor and is clearly visible as bright blue surrounding the *ca.* 10–20 μm oil droplets. The droplets in HFBI–DCBD containing emulsions were much smaller, about 600 nm in diameter. In emulsions containing both NFC and the protein, the droplets were also small and they were coated by a thin layer of cellulose, which was observed by their fluorescence. The fluorescence intensity of droplets containing NFC increased with increased NFC content. As the cellulose concentration was increased, a continuous cellulose matrix was formed in the aqueous phase. Association of the submicron oil droplets to the cellulose fibrils was observed as shown in Fig. 5B and C. Similar structures were observed for CNC (see Fig. S10†).

The stability of the emulsions was studied by following separation of the emulsion phase from the aqueous phase due to creaming. The results are presented as the emulsion stability index (*ESI*), which is calculated from the volume of separated water and the total amount of water as follows.

$$ESI = \left[1 - \frac{V_{\mathrm{w,separated}}}{V_{\mathrm{w,total}}}\right] \times 100\% \quad (1)$$

The equilibrium *ESI*, measured 28 days after formation of the emulsions are shown in Fig. 6. The stability was rechecked under a period of 6 months with no visible change. The stability of the cellulose-containing emulsions was generally dependent on the concentration of nanocellulose, which is probably caused by both the increasing viscosity of the water phase as a function of the nanocellulose content and by the increasing amount of NFC available for encapsulating the oil droplets. The stability of the emulsions was further enhanced by addition of the fusion protein. In Fig. 6A, a comparison of an emulsion series stabilised with varying amount of NFC without protein and with added 1 g l^{-1} of HFBI–DCBD is presented. The data show that full stability of the emulsion could be reached at conditions where the NFC concentration was ~1.25 g l^{-1} and protein concentration 1 g l^{-1}. In the case of plain NFC, the most stable emulsion at the studied concentration range (2 g l^{-1}) had volume of ~80% of the total volume. The protein itself was observed to stabilise emulsions rather well even in the absence of nanocellulose, but the equilibrium volume above 80% could not be reached (see Fig. S11A†). The *ESI* value for the control emulsion containing1 g l^{-1} of HFBI and 1 g l^{-1} NFC was 54%. Stabilisation of emulsions was also studied with CNC, but their ability to stabilise emulsions was much lower (see Fig. S11B†).

From the above observations, two possible reasons for enhanced emulsion stability are proposed. On the one hand, it can be expected that NFC acts as a thickener of the continuous phase slowing down the diffusion of the emulsion droplets when the phases separate due to their density difference. On the other hand, addition of HFBI–DCBD showed a clear enhancement of emulsion stability. One reason for more stable emulsions may be assembly of HFBI–DCBD at the interfaces of the oil droplets, which decreases their size. However, control emulsions containing wild type HFBI and NFC were less stable than the ones containing same amount of NFC and HFBI–DCBD. HFBI

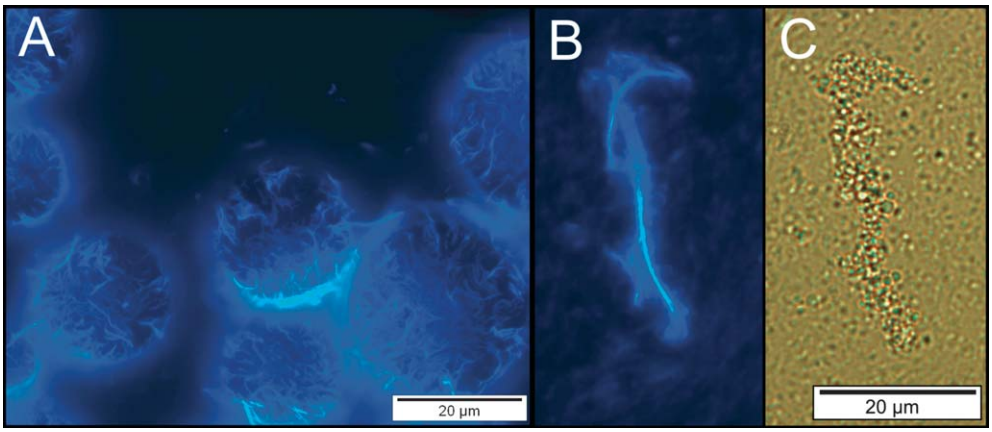

Fig. 5 Epifluorescence microscope images of emulsions. Cellulose has been stained with Calcofluor. (A) An image of emulsion stabilised by 0.1 g l^{-1} of NFC. (B) An image of emulsion stabilised by NFC/HFBI–DCBD. Structures consisting of bundled cellulose fibrils are clearly visible. (C) A bright field microscope image of the same structure. Droplets are seen as small granules following the cellulose structures. Concentrations of NFC and HFBI–DCBD were 0.025 g l^{-1} and 1.0 g l^{-1} respectively.

assembles the oil/water interface, but does not bind to cellulose specifically. These data and the microscope examination of the emulsions indicate that there is interaction between the NFC fibrils and the HFBI–DCBD-coated oil droplets leading to highly stable emulsions. The synergetic effect between the protein and nanocellulose was studied further by examining the measured *ESI* values of emulsions containing NFC and HFBI–DCDB as a function of different variables, such as amount of NFC, total protein, unbound protein and bound protein. The only variable showing a general trend (Fig. 6B) was the amount of HFBI–DCBD bound to NFC, which was calculated from the binding isotherm. For comparison, the inset shows the data plotted against the amount of free protein (see Fig. 6B inset), which shows no clear dependency. According to this observation, the best stabilisation occurs when largest amount of the HFBI–DCBD + NFC complex is present.

Cellulose derivates and modified cellulose have been used widely in emulsions and other drug and food formulations but only few reports on using unmodified cellulose as an emulsion stabiliser have been published.[43–46] The surface of cellulose is hydrophilic, but nanocelluloses (NFC and CNC) have low colloidal stability, leading to bundling of the fibrils and collapse of CNC.[10] Yet, nanocellulose is not amphiphilic and its ability to stabilise emulsions has not been reported widely. Only one report, describing structures similar to our observations where unmodified bacterial nanocellulose has formed a mechanical barrier surrounding oil droplets has been published.[45] The reasons for deposition of mesh of unmodified nanocellulose at the oil/water interface cannot be associated with self-assembly of nanocellulose at the interface, since there was no detectable lowering of interfacial tension in the presence of NFC alone. The reason for oil encapsulation is most probably due to collapse and bundling of

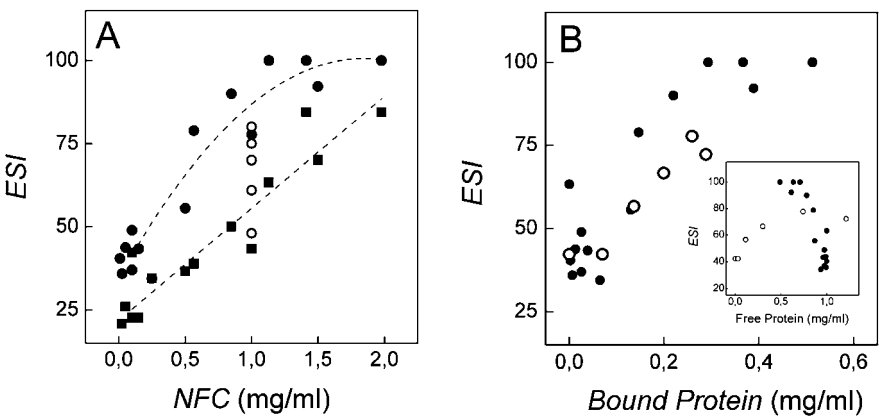

Fig. 6 Emulsion stability indices (*ESI*) of emulsion containing NFC. (A) *ESI* of emulsions stabilised by NFC (filled squares) and combinations of varying amount of NFC and 1 g l^{-1} HFBI–DCBD protein (filled circles) as a function of NFC concentration. A series of emulsions containing 1.0 g l^{-1} of NFC and a varying amount of protein (from 0.1 to 1.5 g l^{-1}) (unfilled circles) showed an intermediate behaviour between pure NFC and the emulsions containing 1.0 g l^{-1} of protein with varying amount of NFC. The dashed lines do not have theoretical meaning but are plotted as a guide to the eye. (B) *ESI* of all emulsions containing combinations of NFC and HFBI–DCBD as a function of bound protein concentration. The data are the same as presented in (A), the emulsions with varying amount of NFC and 1 g l^{-1} HFBI–DCBD protein (filled circles) and the emulsions containing 1.0 g l^{-1} of NFC and a varying amount of protein (unfilled circles). Inset: the same data presented as a function of free protein concentration, showing that there is no meaningful correlation between *ESI* and the amount of free protein.

the nanofibrils at the interface when they were forced in contact with hexadecane during the emulsification.[42] On the other hand, the emulsions high stability might imply the formation of Pickering emulsions, where solid particles assemble at the oil/water interface forming very likely highly stable emulsions.[47]

The behaviour of the HFBI–DCBD containing emulsions shows a difference to emulsions formed by only NFC that can be explained through the dual function of HFBI–DCBD. Formation of oil-droplets by the fusion protein both in the absence and presence of NFC implies that the protein's assembly at the oil/water interface is rapid and that cellulose does not significantly interfere with the assembly or protein orientation. This implies that the structure of the interfacial films in the emulsions is the same two-layered structure that was observed at the flat air/water interface.

3.6 Functionalisation of drug nanoparticles for binding to NFC

The amphiphilic structure of hydrophobin allows it to be used to produce and coat nanoparticles of compounds that have low solubility in aqueous solution, such as some drug compounds.[25] We previously showed when a compound of low solubility in water (here itraconazole (ITR)) was dissolved in a suitable solvent (here tetrahydrofuran (THF)) and then dispersed in an aqueous solution of hydrophobin, nanoparticles were formed (Fig. 7A). Such nanoparticles have many desirable effects such as improved solubility and bioavailability, but the long term stability of the particles can be low, especially in physiological conditions. In Fig. 7B, it can be seen that particles have aggregated and their morphology has changed after five days in aqueous solution.

Next we investigated how a cellulose-binding functionality could be added to the nanoparticles through the use of HFBI–DCBD. The use of HFBI–DCBD resulted in morphologically identical particles as with the HFBII as observed by TEM. The cellulose binding capacity of the nanoparticles was studied by mixing NFC and the nanoparticle solution. HFBI coated nanoparticles were used as the control. It was found that particles associated to NFC, but in a solution dependant manner. At low ionic strength, both HFBI and HFBI–DCBD coated particles were found to associate with NFC (Fig. S12†). However, increasing the ionic strength by adding NaCl up to 300 mM revealed a clear difference between particles with DCBD function and those without, as shown in Fig. 8. Freshly prepared mixtures of particles and NFC showed little difference and

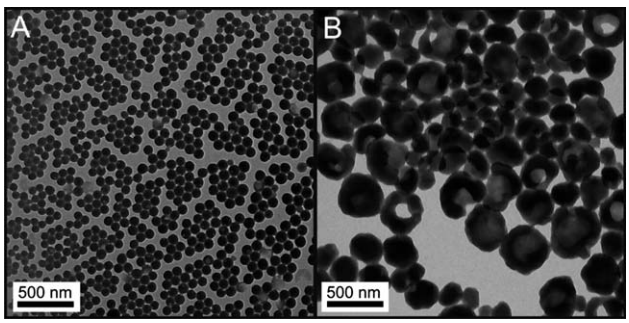

Fig. 7 (A) TEM image of freshly prepared ITR filled nanoparticles coated with hydrophobin (HFBII). (B) The particles are unstable and storage in aqueous solution leads to disruption and disproportionation, as shown here for a five-day old sample.

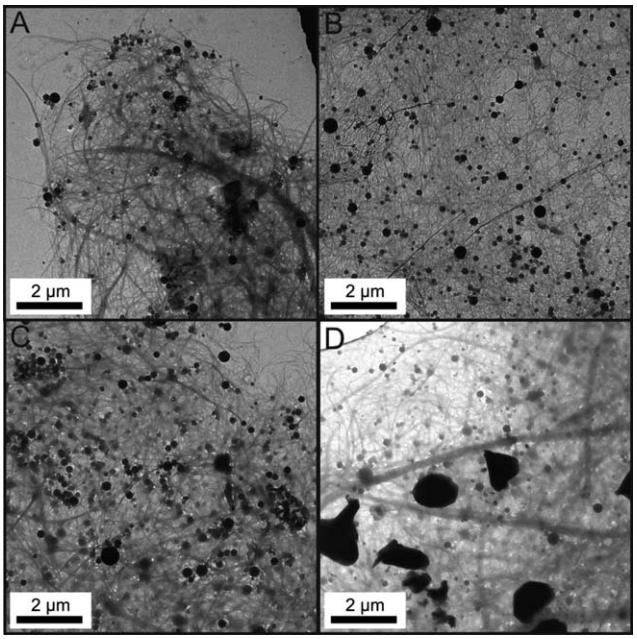

Fig. 8 TEM images of (A) ITR–HFBI–DCBD–NFC sample made in 0.3 M NaCl, (B) ITR–HFBI–NFC sample made in 0.3 M NaCl. Both samples were stored in suspension for 12 days. (C) After storage the morphology of the sample prepared with HFBI–DCBD showed no change, (D) the sample prepared with only HFBI showed strong aggregation.

particles associated with the cellulose could be identified on TEM images. However, upon aging of the samples they behaved distinctly differently. The particles prepared with only HFBI showed strong aggregation and coalescence of particles, with their size growing from *ca.* 50–100 nm to above micrometres after 12 days. In contrast, particles prepared using HFBI–DCBD showed very little change after the same storage. The particles were still attached to the NFC network and well dispersed. Steric stabilisation using polymers has been considered an effective mechanism to shelter drug nanoparticles against aggregation and degradation. It can be more effective than ionic stabilisation because of the high ionic strength and variation in pH in the human body. Therefore, HFBI–DCBD fusion protein ability to bind to NFC with high affinity, regardless of the high ionic concentration, was considered as an integral part of protective matrix for drug nanoparticles.

4 Conclusions

In this work we have demonstrated a way to use specific protein interactions to functionalise nanocellulose. Through this functionalisation, NFC could be self-assembled at the air/water interface, forming thin layers of tightly packed fibrils. The combination of NFC and HFBI–DCBD gave a synergistic effect in the formation and stability of an oil-in-water emulsion. The bifunctional adhesive properties of HFBI were also shown to improve the attachment of drug nanoparticles to NFC and thus improve their stability during storage.

In nature there are innumerable examples of how specific protein interactions control the architecture of cells, tissues and other structures, thereby creating highly functional assemblies.

To achieve a similar level of control of structures is a major goal of materials science and molecular nanotechnology.[48,49] It can be instructive to view the HFBI–DCBD as a block copolymer as it consists of blocks of different functionalities. The interactions of the different blocks lead to self-assembly of the system. In principle such block-copolymers could be produced in a completely non-biological manner if blocks with suitable functionality would be available. However, we are not aware of the existence of non-biological blocks that would function with similar efficiency as the protein blocks used here. We suggest that protein-based block copolymers have the significant advantage that their structures can be engineered on a molecular level in a significantly more precise way than any synthetic system, leading to more specific interactions and higher degree of control. The main drawback of amino acid based systems is that we are currently limited to the 20 naturally occurring ones. However, with the rapid development of molecular and synthetic biology, it is likely that this limitation will be overcome in the future.

The use of genetic engineering allows the production of a vast number of molecular functionalities and combinations thereof, opening an enormous resource for materials engineering on the nano and molecular scale. Nature provides examples of interactions that can be used, such as the ones used in this work. However, we can also fine tune these biological compounds or find entirely new interactions and molecular functions in the laboratory by using methods such as directed evolution.[50] In this way, similar protein-based approaches for structural assembly can be extended to any system, biologic or non-biologic.

Acknowledgements

We thank the Finnish Centre for Nanocellulosic Technologies (Monika Österberg, Eero Kontturi, and Jaakko Pere) for providing the nanocellulose, Riitta Suihkonen for technical assistance, and Dr Tiina Nakari-Setälä is thanked for originally making the HFBI–DCBD construct. The Academy of Finland, the Finnish Funding Agency for Technology and Innovation (TEKES), and the Graduate School for Biomass Refining are thanked for funding.

References

1 I. Siro and D. Plackett, *Cellulose*, 2010, **17**, 459–494.
2 S. J. Eichhorn, A. Dufresne, M. Aranguren, N. E. Marcovich, J. R. Capadona, S. J. Rowan, C. Weder, W. Thielemans, M. Toman, S. Renneckar, W. Gindl, S. Veigel, J. Keckes, H. Yano, K. Abe, M. Nogi, A. N. Nakagaito, A. Mangalam, J. Simonsen, A. S. Benight, A. Bismarck, L. A. Berglund and T. Peijs, *J. Mater. Sci.*, 2010, **45**, 1–33.
3 K. Riehemann, S. W. Schneider, T. A. Luger, B. Godin, M. Ferrari and H. Fuchs, *Angew. Chem., Int. Ed.*, 2009, **48**, 872–897.
4 D. J. Gardner, G. S. Oporto, R. Mills and M. A. S. A. Samir, *J. Adhes. Sci. Technol.*, 2008, **22**, 545–567.
5 D. Klemm, B. Heublein, H. Fink and A. Bohn, *Angew. Chem., Int. Ed.*, 2005, **44**, 3358–3393.
6 M. Pääkkö, M. Ankerfors, H. Kosonen, A. Nykänen, S. Ahola, M. Österberg, J. Ruokolainen, J. Laine, P. T. Larsson, O. Ikkala and T. Lindström, *Biomacromolecules*, 2007, **8**, 1934–1941.
7 A. N. Nakagaito and H. Yano, *Appl. Phys. A: Mater. Sci. Process.*, 2004, **80**, 155–159.
8 M. Ioelovich, *Curr. Trends Polym. Sci.*, 2008, **12**, 43–48.
9 M. Pääkkö, J. Vapaavuori, R. Silvennoinen, H. Kosonen, M. Ankerfors, T. Lindström, L. A. Berglund and O. Ikkala, *Soft Matter*, 2008, **4**, 2492–2499.
10 J. F. Revol, L. Godbout, X. M. Dong, D. G. Gray, H. Chanzy and G. Maret, *Liq. Cryst.*, 1994, **16**, 127–134.
11 R. T. Olsson, M. A. S. Azizi Samir, G. Salazar-Alvarez, L. Belova, V. Ström, L. A. Berglund, O. Ikkala, J. Nogues and U. W. Gedde, *Nat. Nanotechnol.*, 2010, **5**, 584–588.
12 Q. Wu, M. Henriksson, X. Liu and L. A. Berglund, *Biomacromolecules*, 2007, **8**, 3687–3692.
13 L. A. Berglund and T. Peijs, *MRS Bull.*, 2010, **35**, 201–207.
14 C. Gousse, H. Chanzy, G. Excoffier, L. Soubeyrand and E. Fleury, *Polymer*, 2002, **43**, 2645–2651.
15 M. Suzuki, K. Saruwatari, T. Kogure, Y. Yamamoto, T. Nishimura, T. Kato and H. Nagasawa, *Science*, 2009, **325**, 1388–1390.
16 M. Linder and T. T. Teeri, *J. Biotechnol.*, 1997, **57**, 15–28.
17 E. A. Bayer, E. Morag and R. Lamed, *Trends Biotechnol.*, 1994, **12**, 379–386.
18 H. Palonen, M. Tenkanen and M. Linder, *Appl. Environ. Microbiol.*, 1999, **65**, 5229–5233.
19 M. Linder, T. Nevanen, L. Söderholm, O. Bengs and T. T. Teeri, *Biotechnol. Bioeng.*, 1998, **60**, 642–647.
20 M. B. Linder, *Curr. Opin. Colloid Interface Sci.*, 2009, **14**, 356–363.
21 K. Scholtmeijer, J. G. H. Wessels and H. A. B. Wosten, *Appl. Microbiol. Biotechnol.*, 2001, **56**, 1–8.
22 J. G. H. Wessels, *Adv. Microb. Physiol.*, 1997, **38**, 1–45.
23 A. R. Cox, D. L. Aldred and A. B. Russell, *Food Hydrocolloids*, 2008, **23**, 366–376.
24 A. R. Cox, F. Cagnol, A. B. Russell and M. J. Izzard, *Langmuir*, 2007, **23**, 7995–8002.
25 H. K. Valo, P. H. Laaksonen, L. J. Peltonen, M. B. Linder, J. T. Hirvonen and T. J. Laaksonen, *ACS Nano*, 2010, **4**, 1750–1758.
26 C. D. Edgar and D. G. Gray, *Cellulose*, 2003, **10**, 299–306.
27 J. Araki, M. Wada, S. Kuga and T. Okano, *J. Wood Sci.*, 1999, **45**, 258–261.
28 T. Nakari-Setälä, N. Aro, N. Kalkkinen, E. Alatalo and M. Penttilä, *Eur. J. Biochem.*, 1996, **235**, 248–255.
29 T. T. Teeri, P. Lehtovaara, S. Kauppinen, I. Salovuori and J. Knowles, *Gene*, 1987, **51**, 43–52.
30 T. Teeri, I. Salovuori and J. Knowles, *Bio/Technology*, 1983, **1**, 696–699.
31 M. B. Linder, M. Qiao, F. Laumen, K. Selber, T. Hyytiä, T. Nakari-Setälä and M. E. Penttilä, *Biochemistry*, 2004, **43**, 11873–11882.
32 M. Linder, K. Selber, T. Nakari-Setälä, M. Qiao, M. Kula and M. Penttilä, *Biomacromolecules*, 2001, **2**, 511–517.
33 G. E. Means and R. E. Feeney, *Anal. Biochem.*, 1995, **224**, 1–16.
34 N. Jentoft and D. G. Dearborn, *J. Biol. Chem.*, 1979, **254**, 4359–4365.
35 M. Linder, I. Salovuori, L. Ruohonen and T. T. Teeri, *J. Biol. Chem.*, 1996, **271**, 21268–21272.
36 Z. Wang, M. Lienemann, M. Qiau and M. B. Linder, *Langmuir*, 2010, **26**, 8491–8496.
37 G. R. Szilvay, A. Paananen, K. Laurikainen, E. Vuorimaa, H. Lemmetyinen, J. Peltonen and M. B. Linder, *Biochemistry*, 2007, **46**, 2345–2354.
38 J. Hakanpää, G. R. Szilvay, H. Kaljunen, M. Maksimainen, M. Linder and J. Rouvinen, *Protein Sci.*, 2006, **15**, 2129–2140.
39 P. J. Kraulis, G. M. Clore, M. Nilges, T. A. Jones, G. Pettersson, J. Knowles and A. M. Gronenborn, *Biochemistry*, 1989, **28**, 7241–7257.
40 R. Ipsen and J. Otte, *Annu. Trans. Nord. Rheol. Soc.*, 2003, **11**, 89–93.
41 T. B. J. Blijdenstein, P. W. N. de Groot and S. D. Stoyanov, *Soft Matter*, 2010, **6**, 1799–1808.
42 H. Jin, Y. Nishiyama, M. Wada and S. Kuga, *ColloidsSurf., A*, 2004, **240**, 63–67.
43 E. Melzer, J. Kreuter and R. Daniels, *Eur. J. Pharm. Biopharm.*, 2003, **56**, 23–27.
44 L. W. Chan, P. W. S. Heng and L. S. C. Wan, *J. Microencapsulation*, 1997, **14**, 545–555.
45 H. Ougiya, K. Watanabe, Y. Morinaga and F. Yoshinaga, *Biosci., Biotechnol., Biochem.*, 1997, **61**, 1541–1545.
46 M. Andresen and P. Stenius, *J. Dispersion Sci. Technol.*, 2007, **28**, 837–844.
47 R. Aveyard, B. P. Binks and J. H. Clint, *Adv. Colloid Interface Sci.*, 2003, **100–102**, 503–546.
48 M. Muthukumar, C. K. Ober and E. L. Thomas, *Science*, 1997, **277**, 1225–1232.
49 J. Lehn and P. Ball, Supramolecular Chemistry, in The New Chemistry, ed. N. Hall, Cambridge University Press, Cambridge, 2000, pp. 300–351.
50 M. Sarikaya, C. Tamerler, A. K. Jen, K. Schulten and F. Baneyx, *Nat. Mater.*, 2003, **2**, 577–585.

Supporting Information for

Self-Assembly of Cellulose Nanofibrils by Genetically Engineered Fusion Proteins

Suvi Varjonen[1], Päivi Laaksonen[1], Arja Paananen[1], Hanna Valo[2], Hendrik Hähl[3], Timo Laaksonen[2], Markus B. Linder[1*]

[1]Nanobiomaterials, VTT Technical Research Centre of Finland, Tietotie 2, P.O. Box 1000, FI-02044 VTT, Finland, [2]Division of Pharmaceutical Technology, University of Helsinki, P.O. Box 56, FI-00014 University of Helsinki, Finland, [3]Department of Experimental Physics, Saarland University, 66041 Saarbrücken, Germany.

LS films of proteins

Protein monolayers were studied by pipetting a known amount of HFBI and HFBI-DCBD on top of the subphase on a Langmuir trough. The films were compressed to surface pressure 30 mN/m and then picked up on a HOPG substrate. Films were then imaged by AFM (Figure S1).

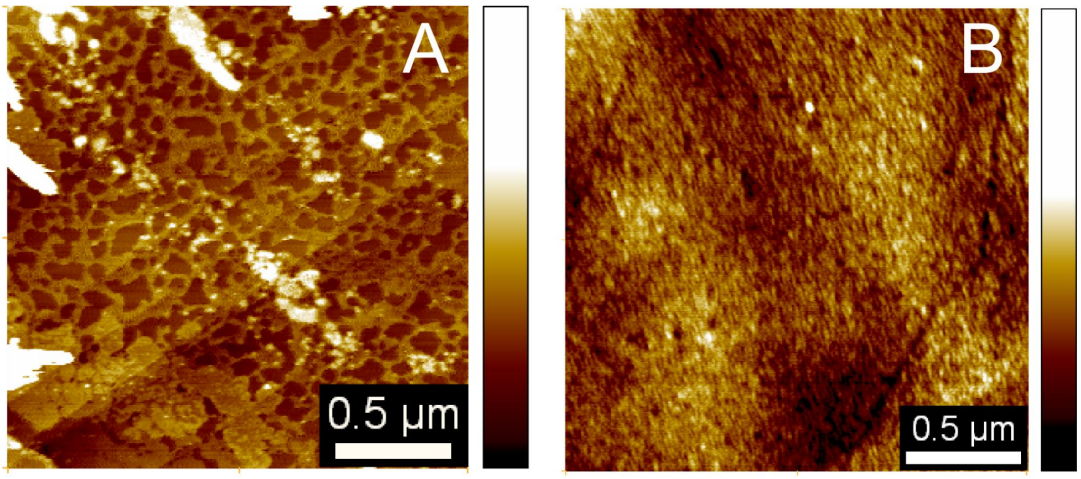

Figure S1. AFM topography images of self-assembled protein films picked up from air/water interface at surface pressure 30 mN/m. A) A monolayer of HFBI. B) A monolayer of HFBI-DCBD.

Ellipsometry

Ellipsometric measurements were carried out using a multi-wavelength ellipsometer (EP3, Nanofilm, Göttingen, Germany) operated at a single wavelength of 532 nm. The device was set up in a PCSA (polarizer-compensator-sample-analyzer) configuration with an angle of incidence of 54° to the surface normal. The air/water interface is realized by a round Teflon trough filled with buffer solution (10 mM acetate buffer, pH 5). Care was taken on choosing the optimal trough diameter, large enough to minimize meniscus curvature in the middle region, where the laser light probes (or: is reflected by) the liquid/air interface. To minimize evaporation, the trough was covered by a hood with a small slit for incident and reflected light beam.

The ellipsometric angles Ψ and Δ were recorded via the nulling ellipsometry principle in two zones[i] thus balancing between measurement time and accuracy of the

measurement. A sampling rate of ca. 1.5 min^{-1} was chosen for the time resolved measurements of the adsorption kinetics.

For the evaluation of the recorded data, an optical box model was applied consisting of the buffer solution (whose refractive index n_s was determined before), the protein film (assumed as homogeneous layer with a fixed refractive index n_f) and the ambient air (simulated as vacuum, $n_v = 1$). This model yields the protein layer thickness d_f as a function of time, yet with a fixed refractive index. The absolute amount of adsorbed protein Γ can be determined with de Feijter's formula

$$\Gamma = d_f \frac{n_f - n_s}{dn/dc} \qquad \text{(Eq S1)}$$

assuming that the refractive index of a protein is a linear function of its concentration, and with dn/dc as the increment of the refractive index due to concentration increase, fixed to a value of 0.183 cm^3g^{-1}.[ii,iii] Since for layer thicknesses smaller than 5 nm it is not possible to determine thickness and refractive index of a layer unambiguously[iv,i], the adsorbed amount Γ is the more reliable value.

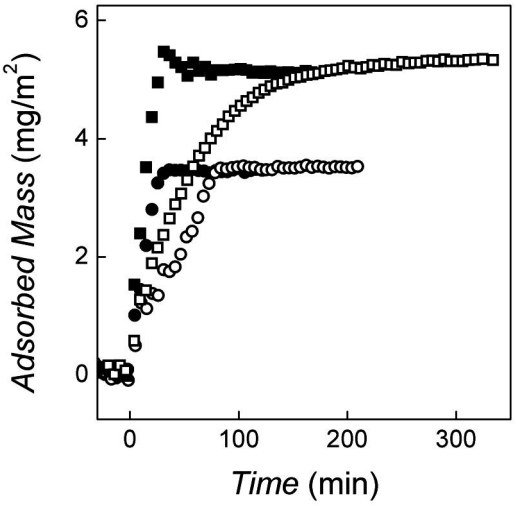

Figure S2. Adsorbed mass of HFBI (circles) and HFBI-DCBD (squares) at the air/water interface as a function of time. Closed symbols correspond to protein concentrations 1 μM and open symbols to 0.5 μM.

Adsorption HFBI and HFBI-DCBD at air/water interface was studied by injecting certain amounts of the proteins into water and measuring the evolution of a surface film. After observing a constant baseline indicating constant ambient conditions, the measurements were started by exchanging 10 ml of the buffer with the protein solution. Complete mixing was achieved by injecting the protein solution into the bulk water at velocities sufficiently high for turbulent flow behavior. Measurement was repeated with protein concentrations 0.5 μM and 1.0 μM (Figure S2.). The final adsorbed masses of HFBI (M = 7.54 kDa) and HFBI-DCBD (18.50 kDa) were ~ 3.5

mg/m^2 and 5.1 ~ mg/m^2, respectively. These correspond to monolayers with mean molecular areas 3.6 nm^2 and 6.0 nm^2.

QCM Analysis of Functionality of the HFB-DCBD Fusion Protein.

Sensograms of the QCM binding studies are shown in Figure S3. The experiment can be divided into three regions, the initial equilibration (baseline), injections of the protein (first vertical line) and CNC (second vertical line). In addition, the surfaces were washed with buffer after each injection. The amount of bound masses were estimated from the frequency change by Sauerbrey equation

$$\Delta m = -\frac{C\Delta f}{n} \qquad \text{(Eq S2)}$$

where C is a constant 17.7 ngHz^{-1}cm^{-2} arising from the properties of the quartz crystal, Δf is the frequency change and n is the overtone of the oscillations.

Injecting of HFBI over a PS surface is known to lead to formation of a monomolecular layer of hydrophobin on the surface. This can be seen for the initial parts of the QCM sensograms for both HFBI and the HFBI-DCBD fusion proteins. Mass of bound HFBI was 200 ng/cm^2 and the HFBI-DCBD bound to a level of 650 ng/cm^2. The bound amounts correspond to mean molecular area of ~ 6.3 nm^2 for HFBI and ~ 4.7 nm^2 for HFBI-DCBD. After protein injection and rinsing, a solution of CNC was injected. The Sauerbrey mass of bound CNC on the HFBI layer was 900 ng/cm^2 and the mass bound to HFBI-DCBD was approximately 3.0 μg/cm^2. Sauerbrey equation is only valid for thin, rigid films, assuming negligible dampening

of the oscillations. The measured dissipation (ΔD) values for CNC binding, however, were significant (12 and 30 × 10^{-6} to HFBI and HFBI-DCBD respectively) and thus their calculated masses are most likely underestimated. The larger the ΔD value, the larger the underestimation is. Nonetheless we can use the Sauerbrey masses as estimations and draw the conclusion that the monolayer of HFBI-DCBD fusion protein has a much higher capability of binding cellulose than wild-type HFBI.

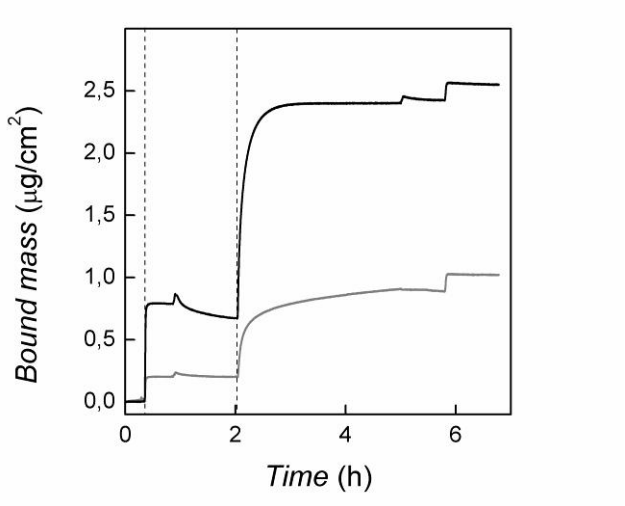

Figure S3. A QCM sensogram of consecutive binding of HFBI (grey line) and HFBI-DCBD (black line) to PS surface and CNC to the resulting protein layers. Injection times of protein and CNC solutions are marked with vertical lines to the image.

Interfacial Shear Rheology

Interfacial shear rheology was measured using TA Instruments AR–G2 controlled stress rheometer equipped with a Du Noüy –ring geometry. The experiments were made on air/water interface at 20 °C. The interfacial films of 0.54 µM HFBI-DCBD with and without nanocellulose were aged in the measuring cup for 20 h. For 1.3 µM

HFBI and HFBI-DCBD the interfacial films were not aged before the measurement, instead the evolution of the interfacial film was measured. Rotational and oscillatory mappings were done before each measurement. The ring was carefully placed onto the interface, immersed into the sample and then brought back onto the interface by automatic control of the geometry height. Three different measurement types were performed for the aged interfacial films: A time dependent experiment at constant frequency (0.1 Hz) and strain (0.01 %), a frequency dependent experiment at constant strain (0.01%) and a strain dependent experiment at constant frequency (0.1 Hz). The frequency dependent experiment was done after the time dependent measurement for the same interfacial film, since the films remained stable. The strain in the above experiments was set to 0.2 % to ensure that the experiments were done in the linear viscoelastic regime. The strain value was selected from a strain dependent experiment where strain was varied from 0.001 to 10 % at a constant 0.1 Hz frequency.

Viscoelastic shear moduli resulting from the adsorption of HFBI and HFBI-DCBD as a function of time are shown in Figure S4. In the case of HFBI–DCBD the G' value after tree hours is almost an order of magnitude lower compared to HFBI. The HFBI–DCBD film forms slower than the film of HFBI in consistency with the observations done by ellipsometry. The G' of HFBI-DCBD starts to increase 75 minutes after starting the measurement , whereas G' of HFBI starts to evolve after ~ 20 minutes.

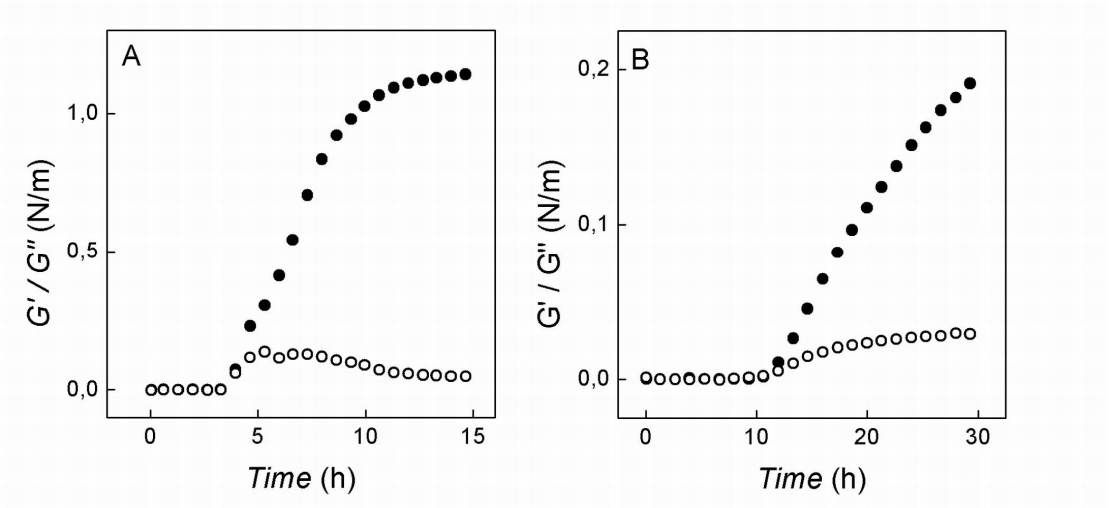

Figure S4. Surface shear moduli of 1.3 µM HFBI (A) and HFBI–DCBD (B) as a function of time. Elastic modulus G' is plotted as the closed circles and viscous modulus G'' as the open circles. Measurements were carried out using constant 0.2 % strain and 0.1 Hz frequency.

Time dependent changes in aged films of 0.54 µM HFBI-DCBD and its mixture with 0.025 mg/ml NFC were studied by exposing them to constant strain and frequency (Figure S5). Addition of NFC to the interface increased the G' values slightly, but the most prominent change was in the increased deviation between parallel experiments done on the NFC containing films. The studied ratio of HFBI-DCBD to NFC represents a situation where ~ 50 % of HFBI-DCBD is associated with NFC; the free HFBI-DCBD concentration being roughly 12 µM and the amount of bound HFBI-DCBD being approximately 5 µmol/g (not fully saturated).

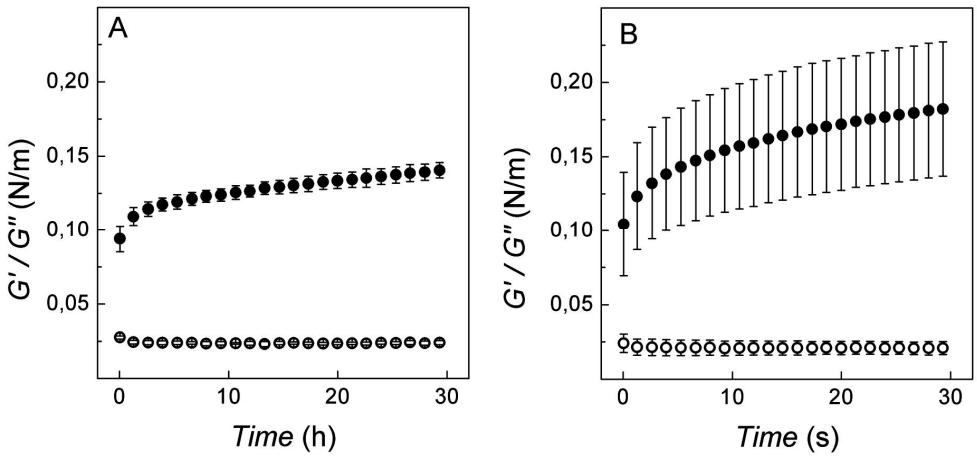

Figure S5. Surface shear moduli of 0.54 µM HFBI-DCBD (A) and 0.54 µM HFBI-DCBD with 0.025 g/l NFC light fraction (B) as a function of time. Elastic modulus G' is plotted as the closed circles and viscous modulus G'' as the open circles. Error bars are calculated from the standard deviation of 3-5 measurements. Measurements were carried out using constant 0.2 % strain and 0.1 Hz frequency.

In the frequency dependent measurement one can note that the G' value of both film types increased monotonically over the investigated frequency range and interfacial shear viscosity |η*| of both samples decreased (Figure S6). Logarithm of the interfacial viscosity is inversely proportional to the frequency on logarithmic scale and indicates shear thinning behavior. Both interfacial shear viscosity and viscoelastic moduli had a power law dependency on frequency (eg. $G' \propto \omega^{n'}$). Power law constants *N*, *n'* and *n''* extracted from the slopes of viscosity, G' and G'' on log-log scale are summarized in table S1.

Table S1. Power law constants for HFBI-DCBD and HFBI-DCBD/NFC films.

	HFBI-DCBD	HFBI-DCBD + NFC
N (viscosity)	-0.86	-0.92
n’	0.12	0.12
n’’	0.07	0.07

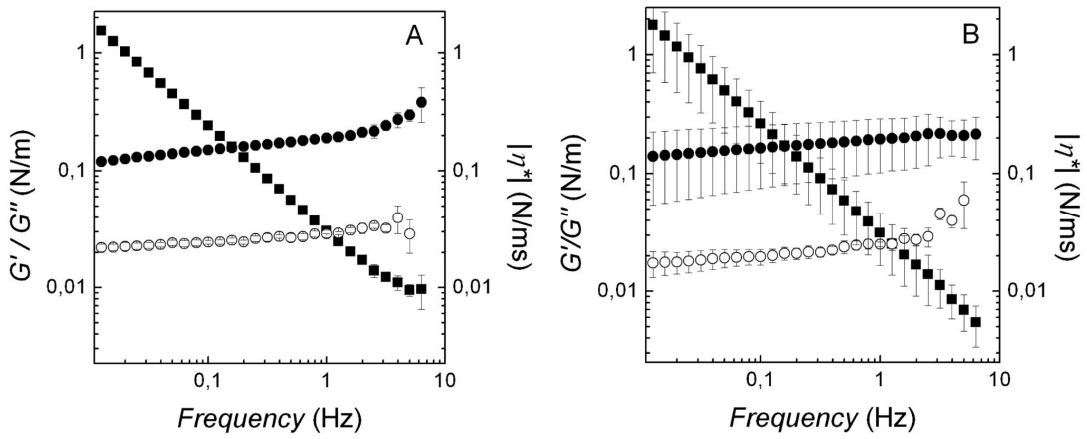

Fig S6. Surface shear moduli and interfacial shear viscosity of 0.54 µM HFBI-DCBD (A) and 0.54 µM HFBI-DCBD with 0.025 mg/ml NFC light fraction (B) as a function of frequency. Elastic modulus G’ is plotted as the closed circles, viscous modulus G’’ as the open circles and interfacial viscosity as squares. Error bars are calculated from the standard deviation of 3-5 measurements. Measurements were carried out using constant 0.2 % strain. The power law constant of the shear viscosity was -0.86 for HFBI-DCBD and -0.92 for the combination.

In the strain dependent measurements one can see the collapse of the viscoelastic moduli at strain 0.25 % (Figure S7). Absolute values of G’ is again higher for the

NFC containing film, but more or less similar effect of increasing strain indicates that NFC does not otherwise affect on the interfacial properties of the protein film.

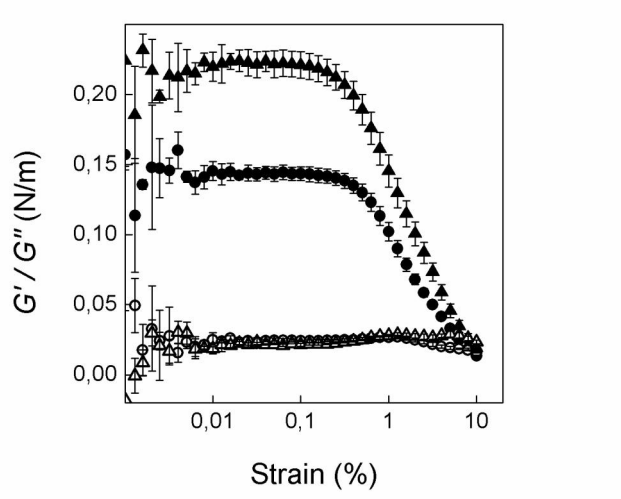

Fig S7. Surface shear moduli of 0.54 µM HFBI–DCBD (circles) and its combination with 0.025 g/l NFC (triangles) as a function of % strain. Elastic modulus G' is plotted as the closed symbols and viscous modulus G'' as the open symbols. Error bars are calculated from the standard deviation of 3-5 measurements. Measurements were carried out using a constant 0.1 Hz frequency.

Emulsification Experiments

Emulsions stabilized with NFC were imaged with optical microscopy. The oil/water interface is clearly visible in bright field images as circular lines (Figure S8A). For verification that an oil-in-water type emulsions were indeed formed, the oil phase was stained with a lipophilic dye (Nile Red) and the emulsion was imaged with a confocal microscopy. In Figure S8B it clearly seen that the droplets were colored and the continuous phase remained unstained. Emulsions stabilized with combinations of

NFC, CNC and HFBI-DCBD were imaged similarly and are presented in Figures S9 and S10. The structure of all emulsions appear more or less similar, but the droplet size in emulsions including HFBI-DCBD was much smaller, only hundreds of nanometers (Figure S9). In Figures S9A, S10A and S10C cellulose has been stained with Calcofluor.

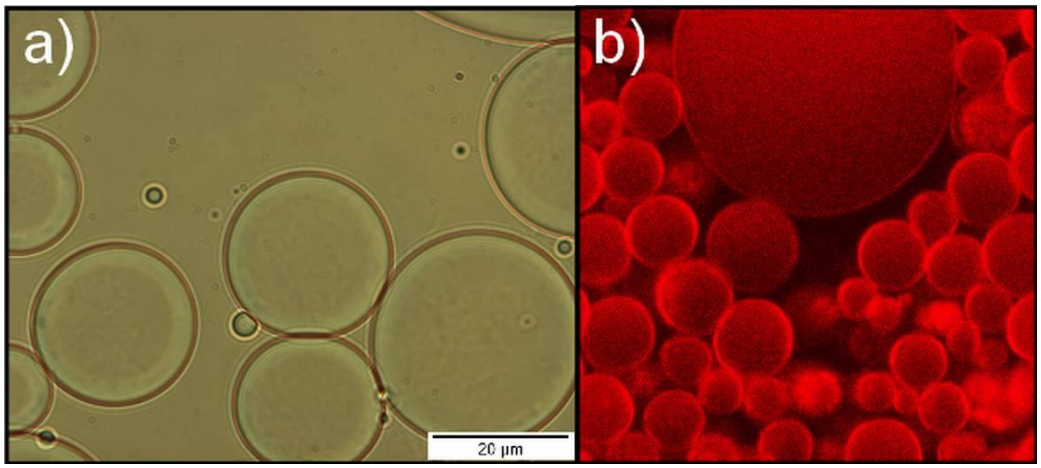

Figure S8. Emulsions stabilized with NFC. A) A bright field microscopy image of emulsion droplets. B) A confocal microscopy image where the oil phase has been stained with Nile Red. Image size is 26 × 26 µm.

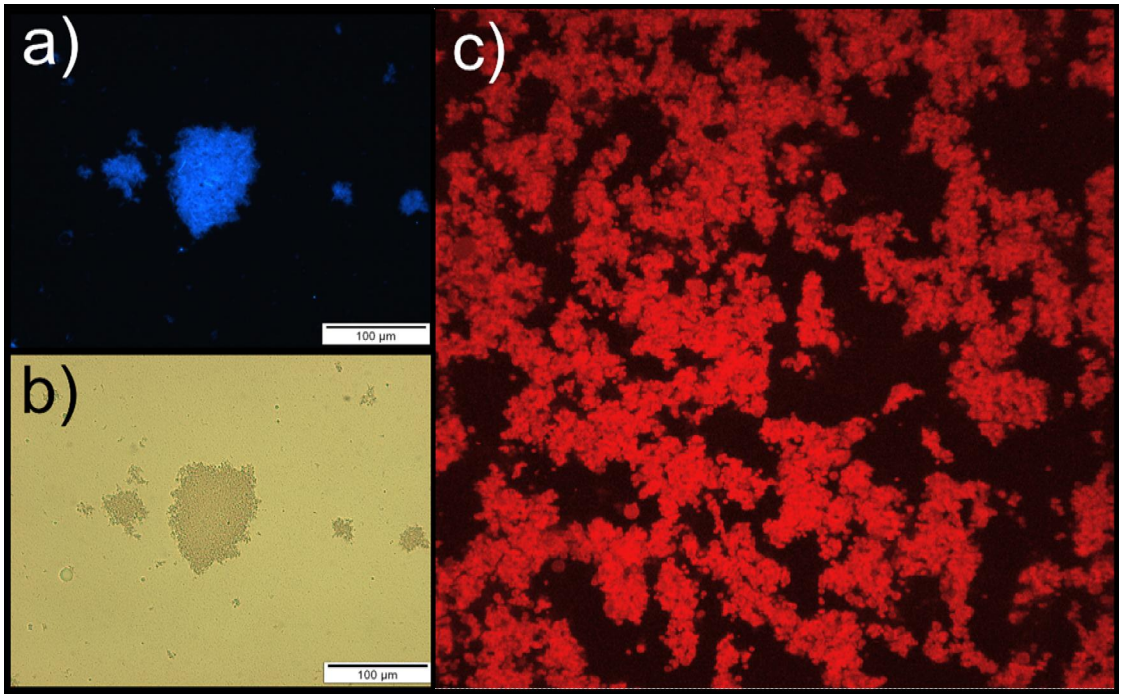

Figure S9. Emulsios stabilized with NFC and HFBI-DCBD. An epifluorescence (A) and a bright field (B) image of emulsion containing nanodroplets associated into larger agglomerates. C) A confocal microscopy image of an emulsion where oil phase has been stained with Nile Red. Image size is 128 × 228 µm.

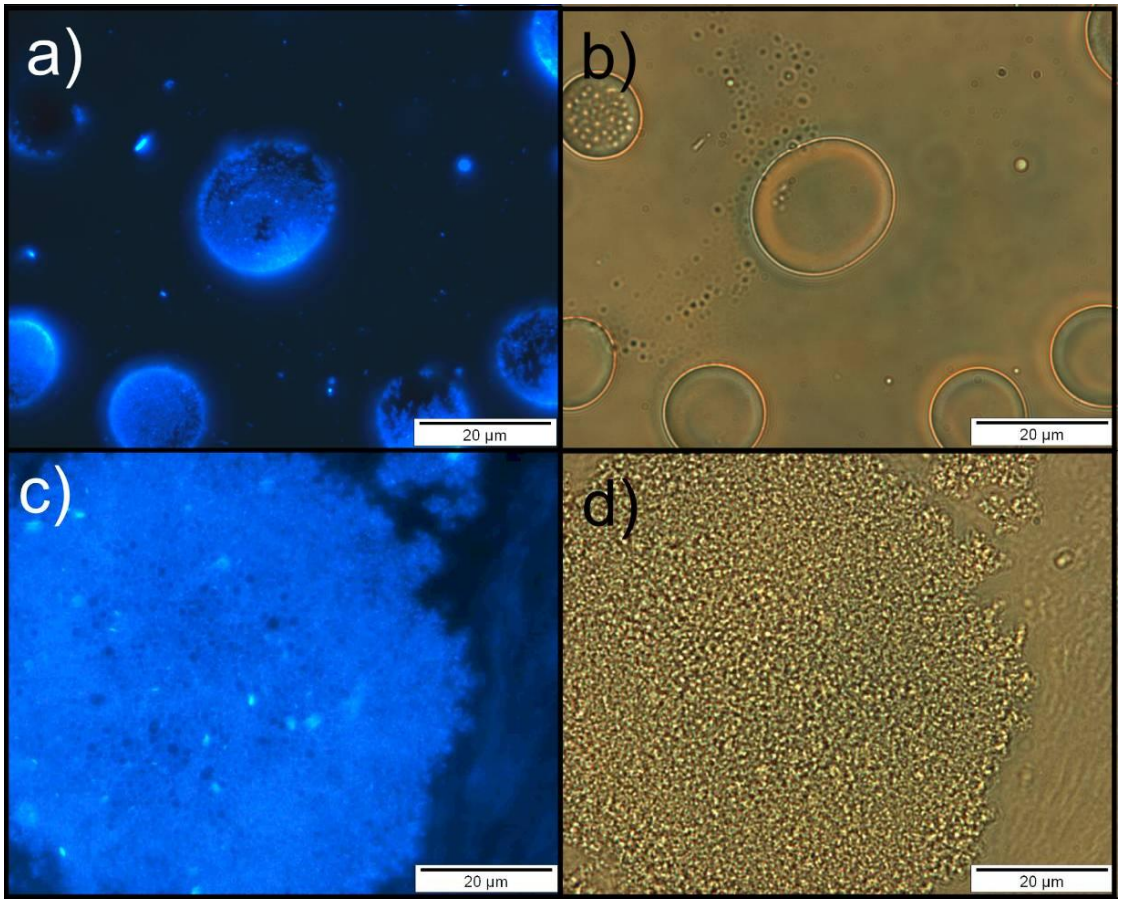

Figure S10. Emulsions stabilized by cellulose nanowhiskers. An epifluorescence (A) and bright field image (B) of an emulsion stabilized by CNC. An epifluorescence (C) and bright field image (D) of an emulsion stabilized by CNC and HFBI-DCBD. Cellulose was stained with Calcofluor.

Stability of emulsions containing only HFBI-DCBD, cellulose nanowhiskers or both in water-hexadecane mixtures was also studied. Emulsion stability indices for these systems are presented in Figure S11. Since hydrophobins are amphiphilic and assemble at oil/water interface, they are also able to stabilize emulsions. In Figure S11A, it is clearly seen that stability of emulsions is increased as the concentration of HFBI-DCBD is increased and reaches a limiting value of about 80 vol-% at concentration 1.5 mg/ml. When cellulose nanowhiskers are added to the system containing 1 mg/ml HFBI-DCBD, a significant decrease in emulsion stability is

observed (Figure S11B). However, compared to emulsions stabilized with only CNC, the combination with protein shows better emulsification ability, by increasing the final volume from about 30 % to 50 %.

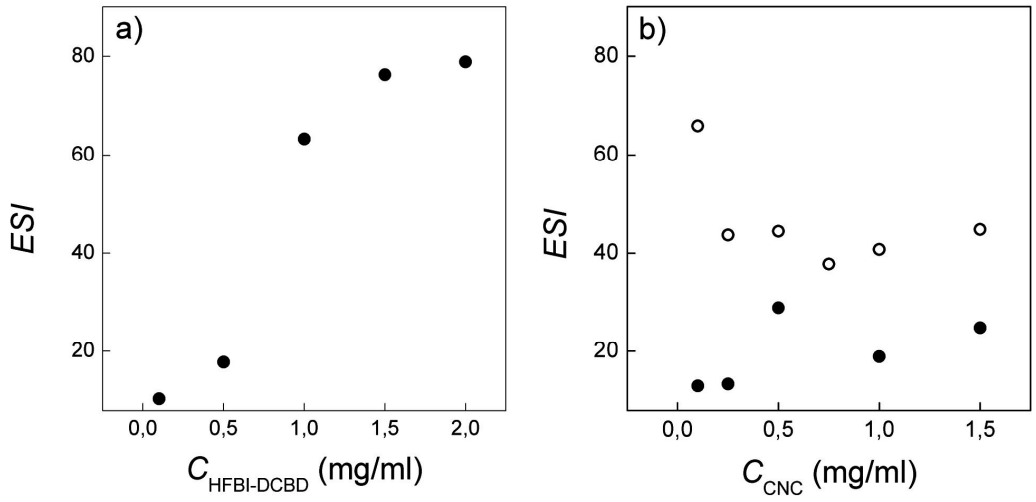

Figure S11. ESI of emulsions stabilized by varying amount of HFBI-DCBD (A), cellulose nanowhiskers (B, black dots) and 1 mg/ml HFBI-DCBD and varying amount of cellulose nanowhiskers (B, open dots).

Binding of Drug Nanoparticles to NFC

For cellulose binding studies, the particles were either prepared with HFBI or HFBI-DCBD coatings. When the nanoparticles were mixed with cellulose, the particles spontaneously attached to the cellulose nanofibrils (Figure S12). This happened with both HFBI and HFBI-DCBD coatings. The lifetime of the particles increased dramatically, and no degradation was observed within 4 weeks. Even though the particles slowly sediment to the bottom of the vial during storage when bound to NFC, they can be readily redispersed with no apparent degradation. The particles are not removed even with mechanical activation, e.g. when subjected to concentration, drying and redispersion in water.

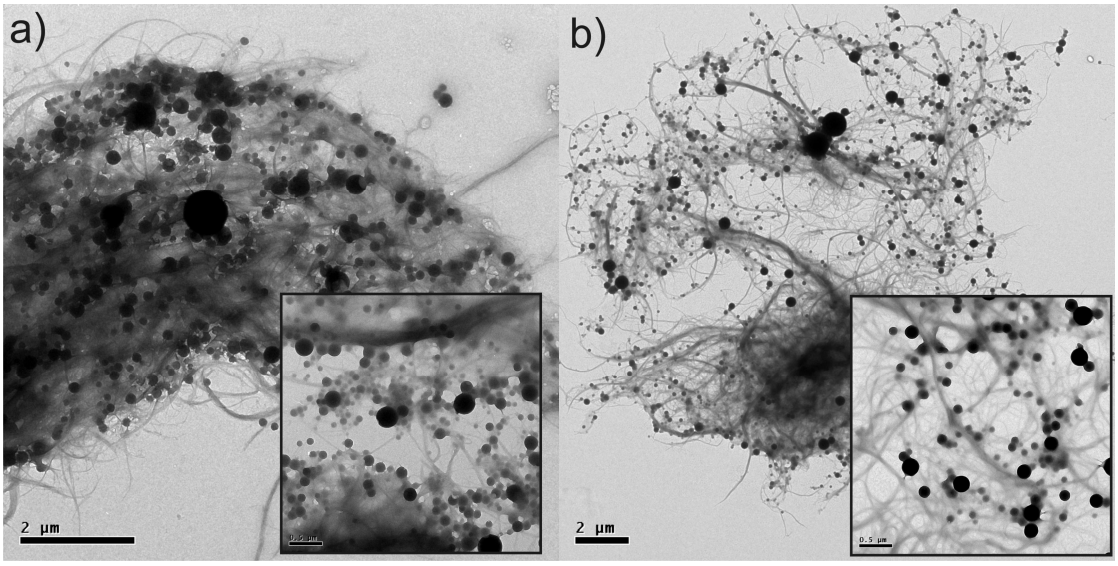

Figure S12. TEM images of a) ITR-HFBI-NFC samples and b) ITR-HFBI-DCBD-NFC samples. Insets show close-ups of the particles.

References

i Tompkins, H. G., & Irene, E. A. (Eds.), Handbook of ellipsometry (2005) Heidelberg, Springer.

ii de Feijter, J. A., Benjamins, J., & Veer, F. A. Ellipsometry as a Tool to Study the Adsorption Behavior of Synthetic and Biopolymers at the Air-Water Interface, Biopolymers (1978) 17, 1759.

iii Ball, V., & Ramsden, J. J. Buffer Dependence of Refractive Index Increments of Protein Solutions. Biopolymers (1998) 46 (7) 489.

iv Azzam, R. M., & Bashara, N. M. Ellipsometry and Polarized Light (1977) Amsterdam: North-Holland.